

## Notation

$N$  := number of points sampled

$$N \sim \Delta x^2$$

$B$  := number of basis functions used in vergini method

$k$  := wavenumber

$E = k^2$  := energy of eigenfunction

$\Delta x$  := orthogonal spacing between sampled points

$$\alpha := k\Delta x$$

$\Omega \in \mathbb{R}^2$  compact domain

$\Gamma = \partial\Omega$  domain boundary

## Introduction

### Motivation

Nodal domains characterize regions of a vibrational surface that move together. The boundaries between nodal domains, known as nodal line are the regions which do not vibrate at all. Understanding the characteristics of nodal domains has potential applications in musical instruments, mechanical engineering, geophysics, astrophysics, and many other areas dealing with wave behavior [Wigman].

The nodal domains studied herein are formulated in terms of quantum mechanical wave functions on Euclidean billiards, a canonical example of quantum chaos. Quantum chaos lies at the intersection of quantum mechanics and chaos theory. The primary signature of chaos in classical systems is a nonlinear (exponential) divergence of paths in phase space of a system. Quantum mechanics however, is entirely linear and quantum chaos deals with energy eigenfunctions of systems, which are constant in time. Thus chaos in quantum systems is manifest in different ways, one of the most studied being wavefunctions in chaotic domains.

Quantum Chaos is...

This matters because...

### Chaotic Billiards

A compact domain  $\Omega \in \mathbb{R}^2$  is chaotic if a classical point-particle follows a trajectory with a positive Lyapunov exponent. A domain  $\Omega$  can be modeled as a potential well

$$V(\mathbf{x}) = \begin{cases} 0 & \text{if } \mathbf{x} \in \mathbb{R}^2 \\ \infty & \text{if } \mathbf{x} \notin \mathbb{R}^2 \end{cases}$$

A quantum wave-particle in the presence of such a potential obeys the Schrödinger equation

$$Eu(\mathbf{x}) = -\frac{\hbar^2}{2m}\nabla^2 u(\mathbf{x}) + V(\mathbf{x})u(\mathbf{x})$$

Setting  $\hbar = m = 1$  and enforcing continuity of  $u(\mathbf{x})$  at the boundary  $\partial\Omega = \Gamma$  reduces this to the Helmholtz equation

$$\begin{cases} (\nabla^2 + k^2)u(\mathbf{x}) = 0 & \text{for } \mathbf{x} \in \Omega \\ u(\mathbf{x}) = 0 & \text{for } \mathbf{x} \in \Gamma \end{cases} \quad (1)$$

where  $k^2 = E$  is the energy of the eigenfunction  $u(\mathbf{x})$  and corresponds to the kinetic energy of the quantum wave-particle.

## Methods

### Vergini Method

Vergini and Saraceno [2] developed a method of computing high energy eigenfunctions of chaotic billiards using a scaling method. The method simultaneously finds all eigenfunctions  $\phi_i(\mathbf{r})$  with energy in a given window  $[E - \Delta E, E + \Delta E]$  by scaling each eigenfunction. The scaled eigenfunctions  $\chi_i(k, \mathbf{r})$  are computed as

$$\chi_i(k, \mathbf{r}) = \phi_i\left(\frac{k}{k_i}\mathbf{r}\right) = \phi_i\left(\mathbf{r} + \frac{\omega_i}{k_i}\mathbf{r}\right)$$

where  $\omega_i = k - k_i$ . This scaling causes all eigenfunctions to fall near a linear subspace of a single basis set  $\{\xi_l\}_{l=1}^B$ , that is

$$\chi_i(k, \mathbf{r}) = \sum_{l=1}^B X_{li}\xi_l(k, \mathbf{r}) + \epsilon_i(\mathbf{r})$$

where  $\epsilon_i(\mathbf{r}) \ll 1$  for sufficiently large  $B$ . Typical values of  $B$  are approximately  $1.5 \frac{k|\Gamma|}{\pi}$ . This fact provides a significant efficiency gain over prior methods because many eigenfunctions can be found by solving a single linear system. The basis functions  $\xi_l(k, \mathbf{r})$  used here are irregular Bessel functions placed along  $\Gamma^+$ , the set of points outside  $\Omega$  whose nearest distance to  $\Gamma$  is  $D$  where  $kD$  is taken to be 7 so that  $D$  is approximately one wavelength. The scaling method runs in  $O(B^3)$  time where  $B$  is the number of basis functions used. The scaling method only computes coefficients of basis functions. [1]

### Counting

Nodal domains are counted by exploring domains pixel by pixel, marking each pixel as “counted” once it has been seen. The searching algorithm used to explore each domain is a hybrid depth- and breadth-first method where for each pixel, the sign of each neighboring pixel is compared to the sign of the nodal domain and if the sign matches, the neighboring pixel is pushed onto a stack. Exploration then continues by popping a pixel off of the stack. This method was chosen so that the signs of all four neighbors (above, below, right, and left) are

known when that pixel is being examined, which is necessary for the adaptive interpolation scheme described below.

Letting  $N$  be the number of points the eigenfunction is sampled at, this method has computational complexity  $O(N)$ . This is because the method performs a fixed number of comparisons for each pixel plus  $O(N)$  total comparisons searching for an unseen nodal domain after a nodal domain has been explored. This algorithm uses an array of  $N$  integers to store, for each pixel, whether it has been counted, which nodal domain it is in, whether or not it is within the boundary of the billiard, and additional information relating to the interpolation method described below. In addition, this method uses a dynamically sized array as a stack whose size it as most the size of the nodal domain being explored and usually only a fraction of that.

## Interpolation

Because sampling eigenfunctions is expensive, we are limited by  $N$  which scales like  $\Delta x^{-2}$ . As a consequence of working with relatively coarsely sampled grids we encounter scenarios where the connectivity of nodal domains is ambiguous (Fig. 1).

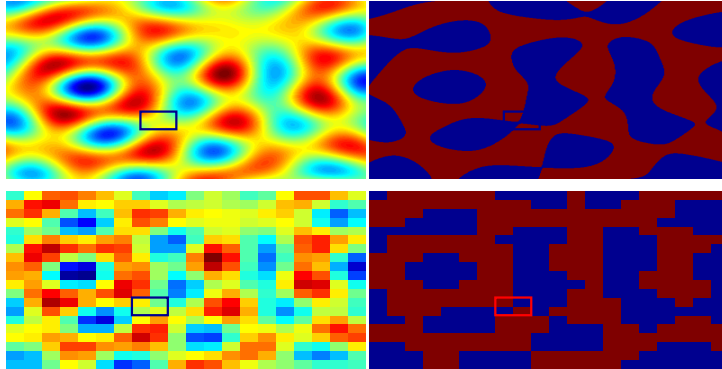


Figure 1: An ambiguity in nodal domain connectivity due to coarse sampling. The ambiguous region is shown with a red box. Top left: high resolution image of an eigenfunction; top right: nodal domains of the same eigenfunction; bottom left: low resolution image of the same eigenfunction; bottom right: nodal domains of low resolution eigenfunction

We resolve such ambiguities by performing an interpolation in the ambiguous region. We interpolate with the functions

$$\xi_i(r, \theta) = \begin{cases} J_i(\alpha r) \sin(i\theta) & \text{if } i > 0 \\ J_i(\alpha r) \cos(|i|\theta) & \text{if } i < 0 \\ J_i(\alpha r) & \text{if } i = 0 \end{cases} \quad (2)$$

where  $J_i(r)$  is a Bessel function (of the first kind) which form a complete orthonormal basis for solutions of (1). We fix a value  $M$  to be the order of the highest order Bessel function, restricting our basis to  $\{\xi_i\}_{|i|\leq M}$ . We construct a surrogate function

$$\tilde{u}(\mathbf{x}) = \sum_{i=-M}^M c_i \xi_i(\mathbf{x})$$

as a local approximation to the eigenfunction  $u(\mathbf{x})$  by fitting the coefficients  $c_i \in \mathbb{R}$  to minimize the error  $\|u - \tilde{u}\|_2$ . This function can then be sampled at a higher resolution within the region in question. We define the sampling ratio of this surrogate function to the original eigenfunction to be  $\rho$ .

Interpolation occurs only between four pixels but uses surrounding values to fit the coefficients  $c_i$ . The selection of which surrounding values to use is termed a stencil. After testing various stencil shapes we selected one using 24 points consisting of a four by four square with two additional points on each side of the square. Error norms for various stencils are shown in figure 2.

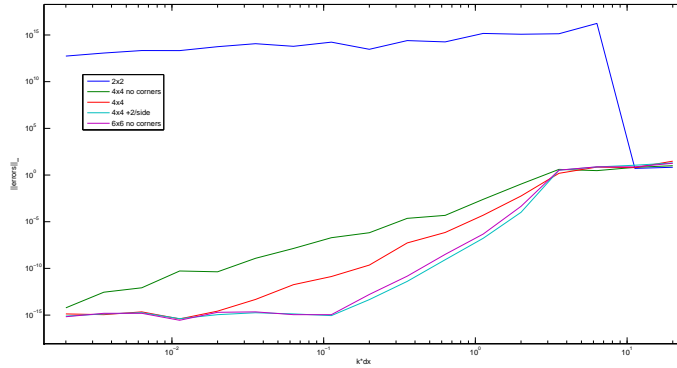


Figure 2: Comparison of error norms of interpolation using several stencil shapes.  $M = 9$

We can construct a single matrix to transform values on a stencil to upsampled values in the center of the stencil, performing the process described above with a single matrix multiplication. We construct the interpolation matrix as

$$U = LH^+$$

Where  $L$  is a matrix which performs an evaluation of Bessel functions at low resolution,  $H$  performs an evaluation of Bessel functions at high resolution and

$A^+$  denotes the pseudoinverse of  $A$ . Specifically,

$$L_{ij} = \begin{cases} J_j(r_i) & \text{for } j = 0 \text{ and } 0 \leq i < 24 \\ J_j(r_i) \sin(j\theta_i) & \text{for } 1 \leq j \leq M \text{ and } 0 \leq i < 24 \\ J_{j-M}(r_i) \cos((j-M)\theta_i) & \text{for } M+1 \leq j \leq 2M+1 \text{ and } 0 \leq i < 24 \end{cases}$$

and

$$U_{ij} = \begin{cases} J_j(r_i) & \text{for } j = 0 \text{ and } 0 \leq i < \gamma \\ J_j(r_i) \sin(j\theta_i) & \text{for } 1 \leq j \leq M \text{ and } 0 \leq i < \gamma \\ J_{j-M}(r_i) \cos((j-M)\theta_i) & \text{for } M+1 \leq j \leq 2M+1 \text{ and } 0 \leq i < \gamma \end{cases}$$

where  $\gamma = (\rho + 1)^2$ ,  $(r_i, \theta_i) = \mathbf{x}_i$  in polar coordinates, and  $\mathbf{x}_i$  are points in the stencil.

The pseudoinverse  $H^+$  is computed using a singular value decomposition as follows,

$$H^+ = V\Sigma^+U^*$$

where  $H = U^*\Sigma V$  is a singular value decomposition of  $H$  and

$$\Sigma_{i,i}^+ = \begin{cases} \Sigma_{i,i}^{-1} & \text{if } \Sigma_{i,i} > \epsilon \\ \Sigma_{i,i} & \text{otherwise} \end{cases}$$

where  $\epsilon = \gamma\epsilon_{double}|\Sigma|$  where  $\epsilon_{double}$  is the difference between 1 and the smallest IEEE double precision floating point number greater than 1. Singular values less than  $\epsilon$  are considered to be zero within working precision.

## Results

## References

- [1] A. Barnett. Asymptotic rate of quantum ergodicity in chaotic euclidean billiards. *Communications in Pure and Applied Mathematics*, 59(10):1457–1488, 2006.
- [2] E. Vergini. Calculation by scaling of highly excited states of billiards. *Physical Review E*, (3):2204–2207, 1995.